JOURNAL OF SOLID STATE CHEMISTRY 67, 235–247 (1987)

Infrared and Raman Study of WO_3 Tungsten Trioxides and WO_3, xH_2O Tungsten Trioxide Hydrates

M. F. DANIEL, B. DESBAT, AND J. C. LASSEGUES*

Laboratoire de Spectroscopie Infrarouge (UA 124 CNRS), Université de Bordeaux I-351, Cours de la Libération, 33405 Talence Cedex, France

AND B. GERAND AND M. FIGLARZ

Laboratoire de Réactivité et de Chimie des Solides (UA 1211 CNRS), Université de Picardie-33, Rue Saint-Leu, 80039 Amiens Cedex, France

Received May 28, 1986

The infrared and Raman spectra of powder samples of WO_3 (monoclinic and hexagonal) and of WO_3, xH_2O ($x = 1,2,\frac{1}{3}$) have been recorded and the most characteristic vibrations are discussed with reference to the available structural data. In particular, a correlation has been established between the force constant and the length of the W–O bond.

Introduction

The structural feature common to the various allotropic modifications of tungsten trioxide and of several of its hydrates is the octahedral oxygen environment of W^{6+}. But the great number of possible arrangements of these octahedra, their distortions and the rather easy hydration of WO_3 either by substitution of one oxygen of the octahedra by H_2O or (and) by intercalation of H_2O between the sheets of the layered structure and not bonded to W^{6+}, lead to a large number of structural situations.

Crystallographic studies have first been performed on some of the numerous stable WO_3 phases which occur between 0 and 1200 K and have more or less distorted ReO_3-type structures. The monoclinic (290–603 K) (*1*) and triclinic (233–290 K) (*2*) phases have been particularly investigated. A schematic projection view of the monoclinic network (m-WO_3) is given in Fig. 1a. It is made of corner-sharing distorted and tilted WO_3 octahedra in which the W atoms are off-center and form three short (1.8 ± 0.1 Å) and three long (2.1 ± 0.1 Å) W–O bonds with the surrounding oxygens.

More recently, a metastable hexagonal modification of WO_3 (h-WO_3) has also been prepared (*3*). It still presents corner-sharing octahedra but with W–O bond lengths of the same order of magnitude (1.92 ± 0.03 Å) (*3*). The projection represented in Fig. 1b shows the large channels which are produced along the hexagonal axis by stacking of infinite planes of WO_6 forming six-mem-

* To whom correspondence should be addressed.

0022-4596/87 $3.00

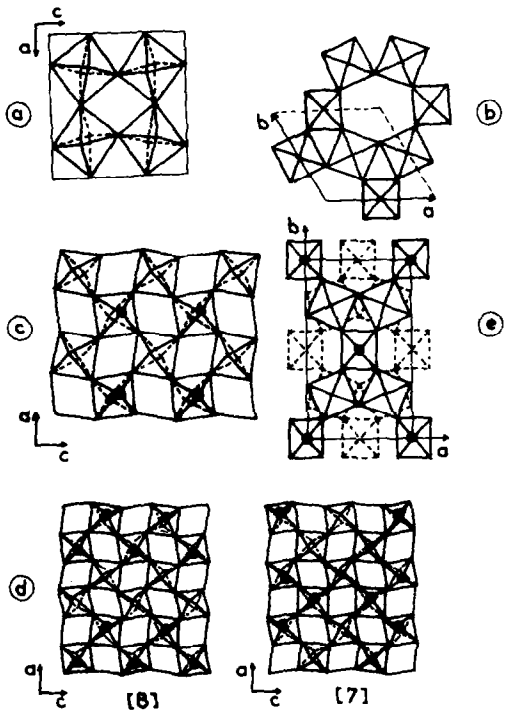

FIG. 1. Schematic representation of some structural features of the studied compounds. (a) m-WO_3 $P2_{1/n}$ (C_{2h}^5), $Z = 8$ (*1*); (b) h-WO_3 $P_{6/mmm}$, $Z = 3$ (*3*); (c) WO_3,H_2O P_{mnb}, $Z = 4$ (*5*); (d) $MoO_3,2H_2O$ $P2_{1/n}$, $Z = 6$ (*7, 8*); (e) WO_3, $\frac{1}{3}H_2O$ F_{mm2}, $Z = 12$ (*9*). The water molecules are indicated by black circles.

bered rings. Actually, this structure corresponds to the W–O skeleton of the hexagonal tungsten bronzes M_xWO_3 (*4*).

The hydrates WO_3, xH_2O involving structural water generally present a distinct structural feature which is the formation of layers of octahedra sharing their four equatorial oxygens with a W–O bond length of about 1.9 Å. When one axial position is occupied by a water molecule, the corresponding W–OH_2 bond is rather long (~2.3 Å) whereas the opposite axial bond is short (~1.7 Å), giving to this terminal bond a double-bond character (this terminal bond will be noted W=O for convenience in the following).

A schematic view of the so-called yellow tungstic acid WO_3, H_2O is given in Fig. 1c. All the octahedra involve a water molecule and the cohesion between the layers is maintained by OH···O hydrogen bonds (*5*).

The structure of the dihydrate WO_3, $2H_2O$ is less well known but there are good indications that it involves layers of octahedra similar to WO_3, H_2O, the second water molecule being intercalated between the layers as in MoO_3, $2H_2O$ (*6–8*). The interlayer distance is thus increased by about 23% (*6*) and the cohesion between the layers is now given by the O–H···O hydrogen bonds formed between coordinated and intercalated H_2O on one hand and between intercalated H_2O and terminal oxygen atoms on the other hand. The two published structural studies of MoO_3, $2H_2O$ (*7, 8*) present only minor differences (Fig. 1d).

The WO_3, $\frac{1}{3}H_2O$ structure involves in a given layer two types of octahedra (Fig. 1e): those which contain a coordinated water molecule with a W–OH_2 bond of 2.1 Å and an opposite terminal W=O bond of 1.8 Å and those which share four oxygen atoms with adjacent octahedra and the two others with octahedra in the upper and lower layers (*9*).

As far as we know, the more detailed vibrational study of the WO_3 stable phases has been reported by Salje (*10*). From the Raman spectra between −180 and 290°C, this author gives an interpretation of the phonon spectra of the phases of higher symmetry in terms of group theory and discusses the critical behaviour of some normal modes at the phase transitions.

Most of the other spectroscopic studies of WO_3 and WO_3, xH_2O deal with powders or more or less crystallized films (*9, 11–21*). The analysis is based on the fact that, as in many other octahedral systems, the WO_6 stretching and bending vibrations occur invariably in the 950–600 and 400–200 cm^{-1} regions, respectively, with subclassifications for the short terminal W=O bonds

and the bridging W—O—W or 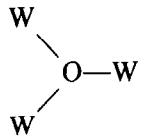 bonds. This concept of group frequency has been developed for example by Cotton and Wing (*22*) or Beattie and Gilson (*15*) for a number of oxides.

More recently, some specific classes of oxides have been more thoroughly investigated with the aim either to establish correlations between force constants and bond lengths as in molybdenum oxides (*22, 23*) or transferable force fields as in vanadium oxides (*24, 25*).

Unfortunately, single crystals are not readily available for *h*-WO_3 and WO_3, xH_2O to perform detailed infrared and Raman studies and force field calculations. The aim of this study is to provide an unambiguous fingerprint of the different compounds. In Raman spectroscopy, great care has been taken to avoid any problem of degradation by the laser. In infrared spectroscopy, the published results are rather scarce and we have tried in particular to characterize adsorbed and structural water.

Experimental Conditions

Monoclinic WO_3 and WO_3, H_2O are commercially available (Merck). The latter was also prepared for verification by the Freedman method (*26*). WO_3, $2H_2O$ was prepared according to the Freedman (*26*) or Furusawa (*27*) methods. The preparations of *h*-WO_3 and WO_3, $\frac{1}{3}H_2O$ have been described previously (*3, 9*).

The Raman spectra have been obtained from the powders either sealed in a glass tube or simply deposited on a metallic support. A spectrometer RAMANOR (Jobin et Yvon) equipped with an argon ionized laser has been used. As explained below, the powder and wavelength of the laser have been chosen according to the stability of the various compounds.

The infrared spectra have been recorded on a Perkin-Elmer 983 G double-beam spectrometer by using nujol or hexachlorobutadiene mulls contained between two cesium iodide windows.

A preliminary experiment has also been attempted by inelastic neutron scattering (INS) on WO_3, H_2O to see to what extent this technique can bring complementary information on the water low-frequency vibrations and rotational dynamics. The IN6 spectrometer (*28*) of the Laue-Langevin Institute was used at an incident wavelength of 5.1 Å. The sample was contained between two thin flat aluminium foils. Standard correction programs (*29*) were used to extract the scattering law $S(Q,\omega)$ in the elastic/quasielastic scattering region and the frequency distribution function $p(\omega) = [\omega^2\ [S(Q,\omega/Q^2]_{Q\to 0}$ for the inelastic part of the spectrum. The resolution depends very much on the energy transfer $\hbar\omega$. It is of the order of 0.5 cm^{-1} (FWHH) at $\hbar\omega = 0$ but deteriorates quickly for high neutron energy gains (~30 cm^{-1} at $\hbar\omega = 150$ cm^{-1}). This has to be kept in mind for the comparison with the optical spectra taken with an average resolution of 3 cm^{-1}.

Results

Infrared or (and) Raman spectra of the stable room temperature *m*-WO_3 phase have already been reported a number of times (*10–21*). A general agreement exists between these different results and those presented in Fig. 2 and Table I. However, small differences occur in the profile of the intense infrared band between 600 and 950 cm^{-1} (*10–12, 14, 16, 18, 19*). As shown in Fig. 2 they may come from different sampling conditions. Particle size and host medium effects are likely to produce spectral distortions and broadenings (*30, 31*).

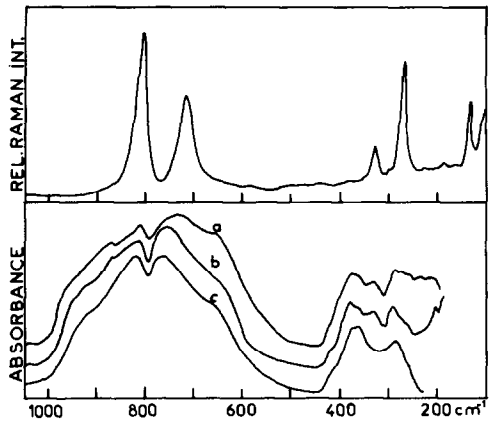

FIG. 2. Raman and infrared spectra of m-WO_3 at room temperature. The latter are obtained by deposition on a silicon window (a), in a nujol mull (b), or in KBr (c).

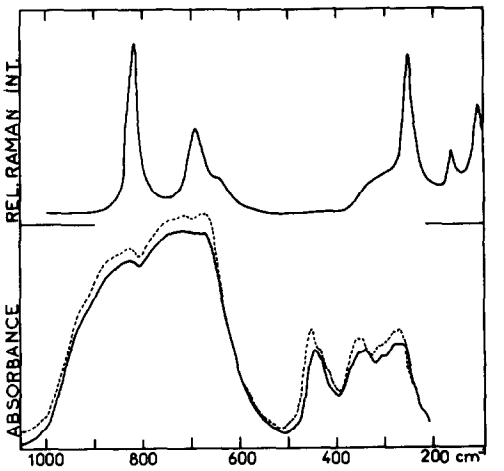

FIG. 3. Raman and infrared spectra of h-WO_3 at room temperature (full line) and at 77 K.

The situation was less clear for h-WO_3 and our results differ markedly from the published ones (*19, 21*). As shown in Fig. 3 the infrared and Raman spectra of h-WO_3 are definitely distinct from those of m-WO_3 provided the Raman spectra are obtained at low laser power (<100 mW) to avoid the transformation of this metastable phase into m-WO_3 (*21*) or into an ill-defined intermediate state (*19*).

No trace of water was detected by infrared spectroscopy neither for m-WO_3 nor for h-WO_3 in such a way that the spectra above 1200 cm^{-1} are not given.

This is not the case of course for the hydrates WO_3, H_2O; WO_3, $2H_2O$; and WO_3, $\frac{1}{3}H_2O$ the infrared spectra of which are compared between 4000 and 1200 cm^{-1} in Fig. 4. They are in general agreement with the few results previously published (*9, 11, 12, 17, 32*). However, some minor but interesting differences must be pointed out. The infrared spectrum of the so-called "white tungstic acid" given by Spitzin and Kabanow (*11*) and supposed to correspond to the formula $(WO)_x(OH)_{4x} \cdot yH_2O$ differs clearly from WO_3, $2H_2O$ by the presence of bands at 1410, 1200, and 1100 cm^{-1}.

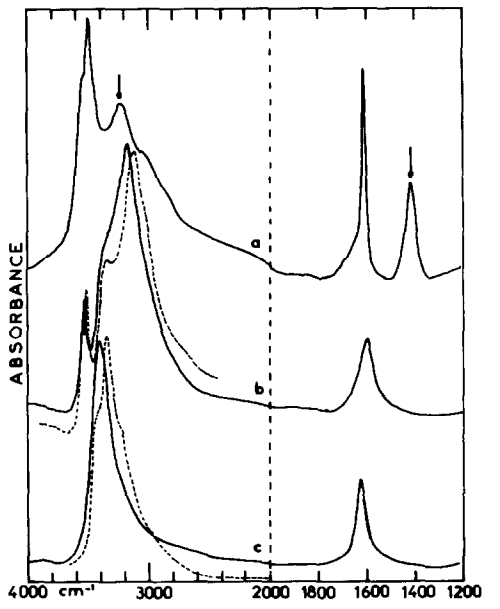

FIG. 4. Infrared spectra of WO_3, $\frac{1}{3}H_2O$ (a), $WO_3,2H_2O$ (b), and WO_3,H_2O (c) in the ν(OH) and δ(OH) spectral region at room temperature. When important modifications occur at 77 K, they are given by broken lines. The bands indicated by arrows for WO_3, $\frac{1}{3}H_2O$ disappear after degassing at 448 K (*9*).

TABLE I

CHARACTERISTIC FREQUENCIES (cm^{-1}) OF THE WO_3 AND WO_3,xH_2O COMPOUNDS[a]

	m-WO_3		WO_3,H_2O		$WO_3,2H_2O$		*h*-WO_3		$WO_3,\frac{1}{3}H_2O$	
	IR	R	IR	R	IR	R	IR	R	IR	R
			3390 (3430)		3530 (3550)				3550	
ν(OH)			(3340)		(3510)				3495	
			3170 (3220)		3370 (3360)					
					3160 (3120)				3220*	
δ(OH)			1620 (1620)		1595 (1587)				1609	
									1410*	
					1007 (1009)				1000	945 (948)
ν(W=O)			948	948 (947)	945 (945)	960			950	
					918 (918)					
	870	807			(820)		830	817	820	805 (805)
	815				700 (712)		735	690	740	
ν(O—W—O)	755		730		680 (685)	685	700		710	
	665	715	680	645 (638)	610 (600)	662	670	645	660	680 (683)
					(494)					
			420 (419)		(474)					
Water			370 (390)		427 (431)					
librations			330 (330)		400 (396)					
					377 (379)					
					355 (354)					
ν(W—OH_2)			370 (373)	377	377 (379)	380				320 (325)
	380	434					442 (446)		420 (425)	
	330	327	330 (330)		326 (334)		(429)			
δ(O—W—O)	280	273	270 (280)	(270)	(315)		(411)			
ν(W—O—W)	225	218		253 (250)	(300)		350 (350)		360 (364)	
				235	273 (273)	268	337 (341)	320	(338)	320
				192 (200)	(240)	235	303 (307)		(296)	
					(229)	210	270 (265)	253	270 (277)	255
					(202)					
		187		(170)						190
		134		150 (150)				162		155
Lattice		93		90 (98)		110		108		
modes		71		50 (55)				80		
		61		36						
		44								
		34								

[a] The infrared and Raman spectra are recorded at room temperature and in a few cases at liquid nitrogen temperature (values between parentheses). The ν(OH) and δ(OH) frequencies are those of water molecules except those indicated by an asterisk which correspond to hydroxyl groups. Some frequencies appear twice when their assignment is uncertain, for example, between water librations and octahedra deformations.

Similarly, the spectrum of $WO_3,\frac{1}{3}H_2O$ presented in Fig. 4 corresponds to a sample not completely desorbed by vacuum treatment and is polluted by adsorbed water or hydroxyl groups as indicated by bands at 3220 and 1410 cm^{-1} which disappear after a careful thermal treatment at 175°C (*9, 33*).

Thus, it appears that some care must be taken in the preparation of these hydrates, the infrared spectra in the ν(OH) and δ(OH)

regions providing the more severe test of composition and purity.

Raman scattering is less efficient in this spectral range but gives specific informations for each hydrate below 1200 cm^{-1}. The spectra of WO_3,H_2O; $WO_3,2H_2O$; and $WO_3,\frac{1}{3}H_2O$ are, respectively, reported in Fig. 5, 6, and 7 and compared with the infrared ones. In the case of WO_3,H_2O, we have also reported the INS spectrum at 349 K.

Again great care was taken to avoid decomposition by the laser. Above 100 mW with the 4880 Å exciting line, the hydrates transform irreversibly to *m*-WO_3. This explains why WO_3,H_2O has for example been indexed with the frequencies of *m*-WO_3 in Ref. (*21*).

For $WO_3,2H_2O$, we have chosen to present the spectra of the sample obtained by the Furusawa method (*27*) because they are better defined than those corresponding to the Freedman preparation (*26*). Although no difference is detected in the X-ray diffractograms, the microcrystals obtained by the Furusawa method have effectively been shown to be of better quality and larger size (*32*).

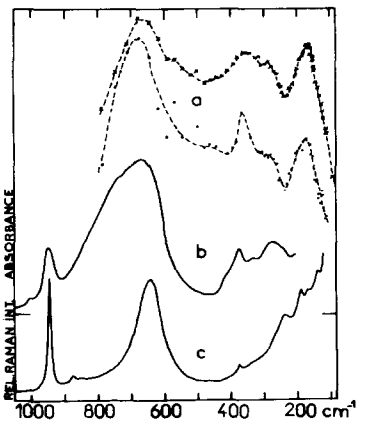

FIG. 5. Comparison of the INS (a), infrared (b), and Raman (c) spectra of WO_3,H_2O. The former taken at 348 K are represented under the form of the function $\omega^2\,[S(Q,\omega)/Q^2]$ summed over all the scattering angles (×) or, after extrapolation to $Q = 0$, in the $p(\omega)$ representation (●) to show the negligible dispersion of the observed modes.

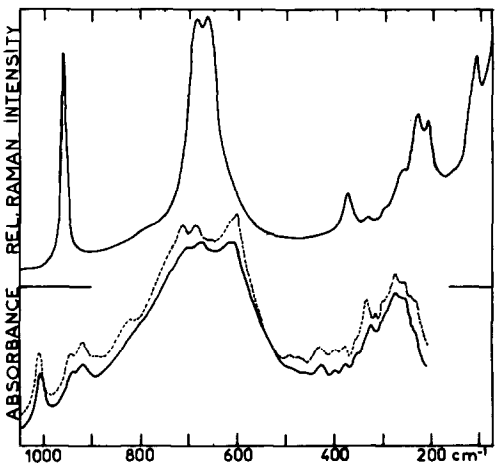

FIG. 6. Raman and infrared spectra of WO_3, $2H_2O$ at room temperature (full line) and at 77 K.

Discussion

(1) Monoclinic WO_3

Three main regions appear for the WO_3 vibrations at 900–600, 400–200, and below 200 cm^{-1}. As already established (*10–22*),

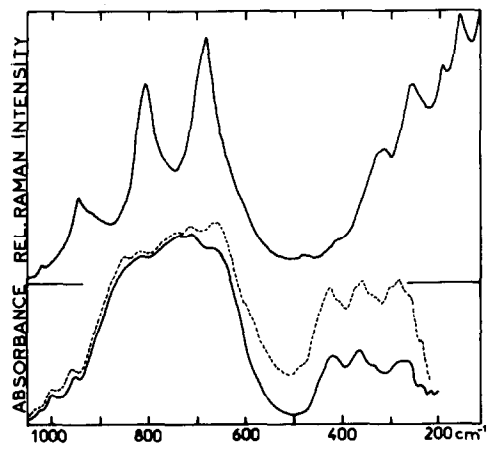

FIG. 7. Raman and infrared spectra of $WO_3,\frac{1}{3}H_2O$ at room temperature (full line) and at 77 K.

they correspond, respectively, to the stretching, deformation and lattice modes. In a more detailed analysis using group theory (*10, 14*) it has been shown that in an ideal ReO_3-type structure of space group O_h^1, there are only two infrared active T_{1u} modes. The distortion of the octahedra and the considerable lowering of the symmetry in the real monoclinic situation ($O_h^1 \rightarrow C_{2h}^5$) leads of course to a great number of active modes in both spectroscopies. However, the strong intensity of the A_g and B_g modes in Raman gives rise to rather well defined lines whereas broad adsorptions are observed in the infrared with a larger frequency distribution.

For a more complete vibrational analysis of *m*-WO_3, force field calculations based on infrared and Raman data obtained on a single crystal would be needed. But this would constitute a separate and complex study in itself.

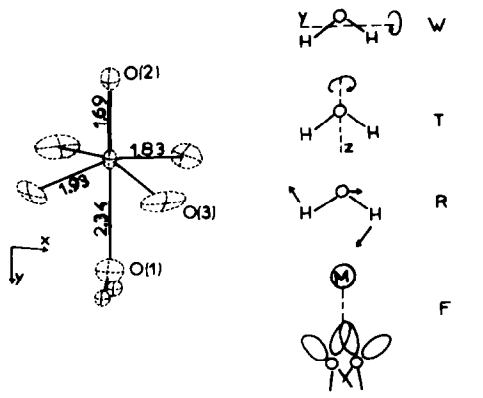

FIG. 8. Schematic representation of the WO_3,H_2O octahedron. In the temperature factor: $T = \exp\{-2\pi^2(U_{11}a^*h^2+\cdots+2U_{12}a^*b^*hk+\cdots)\}$, the diagonal terms U_{11},U_{22},U_{33} of the three kinds of oxygen atoms ($\times 100$) are, respectively, $O_{(1)}$: 3.4,2.4,1.5; $O_{(2)}$: 1.7,2.0,1.5; $O_{(3)}$: 6.1,2.0, and 7.4. The diagonal terms are small or zero (see Table 2 of Ref. (*5*)). The wagging (W), twisting (T), rocking (R) and flipping (F) modes of the water molecule are also represented with the usual convention for the *x,y,z* axes which is different from that used for the tetrahedron.

(2) WO_3,H_2O

A recent structural investigation of tungstite (*5*), a natural compound which has been shown to give a diffraction pattern identical to that of WO_3,H_2O, allows a better understanding of the infrared and Raman spectra. Some characteristic distances of the (WO_5OH_2) octahedron are reported in Fig. 8 together with a few thermal parameters for the oxygen atoms taken from Table 2 of Ref. (*5*).

The large number of vibrational degrees of freedom having their main components in the layer plane explains the large thermal ellipsoids of the bridging oxygens and their anisotropy. The two axial oxygens are concerned by a smaller number of vibrations but one can note that the major axis of the water oxygen thermal ellipsoid is perpendicular to the molecular plane.

It is easy to assign the 948-cm^{-1} band present in the infrared and Raman spectra to the stretching mode of the terminal W=O bond (*8, 12, 15–21*). The stretching modes ν(OWO) of the bridging oxygens occur between 600 and 750 cm^{-1} according to a spectral density very different from that of *m*-WO_3 as expected from the two-dimensional character of WO_3,H_2O compared with the three-dimensional *m*-WO_3 network. In particular, the Raman spectrum exhibits only a broad featureless band centered at 645 cm^{-1} instead of two relatively narrow lines at 807 and 715 cm^{-1} in *m*-WO_3. Marked differences also occur in the 200- to 450-cm region where δ(OWO) modes mainly contribute.

The stretching and bending vibrations of the water molecule are also easily identified respectively around 3390 and 1620 cm^{-1}. The former splits into three components at 77 K. The low-frequency shoulder at ~3220 cm^{-1} can be assigned to the overtone 2δ(OH) of the δ(OH) mode at 1620 cm^{-1} which is little temperature dependent. The 3430- and 3340-cm^{-1} splitting can be described in terms of antisymmetric and sym-

metric OH stretching although the structure indicates the existence of two different hydrogen bond lengths O–H···O = 2.87 and 2.97 Å (*5*).

The translational and librational motions of the water molecule are more difficult to detect. Figure 8 gives a schematic representation of these motions.

The translational motion T_Z or $\nu(M\text{–}OH_2)$ is usually found in the spectral range 300–400 cm^{-1} for trigonally bonded water (*34*).

A normal coordinate analysis of the anion $W_6O_{19}^{2-}$ gives a ratio of force constants for the terminal, bridging, and "central" metal–oxygen bonds of 8 : 4 : 1 (*35*).

Although WO_3,H_2O is a rather different system, on the basis of a $\nu(W{=}O)$ frequency of 950 cm^{-1} (972 for $W_6O_{19}^{2-}$), values of 670 and 335 cm^{-1} are deduced, respectively, for the $\nu(O\text{–}W\text{–}O)$ and $\nu(W\text{–}OH_2)$ frequencies.

The infrared, Raman, and INS spectra effectively present a band at ~370 cm^{-1} which can be assigned to $\nu(W\text{–}OH_2)$. Indeed, it is reasonable to think that this vibration, which involves rather large amplitude motions of the hydrogens in a well-defined mode of the (WO_5OH_2) octahedron, gives rise to a prominent INS peak and to a rather well defined infrared band (Fig. 5).

As shown by the comparison of the infrared and Raman spectra of a large number of hydrates (*34*), general rules can hardly be invoked for the prediction of the librations of the water molecule. The intensities follow roughly the sequence wag>rock >twist, the latter being even infrared inactive for C_{2v} symmetry. The actual site symmetry of H_2O in WO_3,H_2O is C_s but the twisting must remain of very weak intensity. The frequencies can fall in the range 200–700 cm^{-1} according to the nature and strength of the water coordination. Furthermore, the librations can be coupled to other motions of the octahedron and be broadened by dynamical disorder.

Shoulders or weak bands are observed in the infrared spectrum (Fig. 5) at 420,370, and 330 cm^{-1}. One of the librations could even occur on the low-frequency side of the strong absorption at 600–800 cm^{-1}, explaining the strong intensity of the INS band at 690 cm^{-1} (Fig. 5). However, deuteration effects would be needed for a precise assignment since the low-temperature spectra do not provide more detailed features.

The presence of dynamical disorder of the water molecule is shown by observation of quasielastic scattering in the neutron spectra (Fig. 9). It can only be due to some kind of reorientational motion.

This profile can satisfactorily be reproduced by the simple expression

$$S(Q,\omega) \propto \left\{A(Q)\,\delta(\omega) + \frac{1}{\pi}\,[1-A(Q)]\,\frac{\sigma}{\omega^2+\sigma^2}\right\} + a \quad (1)$$

where the elastic incoherent structure factor (EISF) $A(Q)$ is given by the expression $\frac{1}{2}$ [1 + (sin Qd)/Qd], corresponding to a model of instantaneous proton jumps between two positions separated by the distance d (*36*); a is a flat background introduced to correct from inelastic contributions.

The width of the Lorentzian σ (HWHH) fitted independently for each angle was found nearly constant at 0.18 ± 0.02 meV, corresponding to a correlation time $\tau = 2/\sigma$ of ~7 10^{-12} sec.

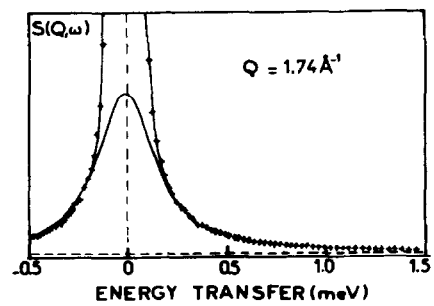

FIG. 9. Typical quasielastic neutron scattering spectrum of WO_3,H_2O at 348 K.

The EISF value remains rather high (0.85 at $Q = 2$ Å^1), implying either the non equivalence of the water molecules, some being seen as fixed and other as mobile, or a special kind of motion giving a rather short distance (~0.7 Å) between the two positions explored by a given proton. According to previous hypotheses on other hydrates, the water molecule is sometimes supposed to execute a flipping motion corresponding to the alternative orientation of each oxygen lone pair towards the metal (Fig. 8) (*37, 38*). The thermal ellipsoid of the water oxygen in WO_3,H_2O is indeed very anisotropic, with its long axis perpendicular to the water molecule plane (*5*).

A jump distance of 0.7 Å would be anyway more in agreement with a flipping motion than with oscillations about the x axis (~0.2 Å) or reorientations about the z axis (~1.5 Å) (Fig. 8).

Further experiments would be necessary to precise the water dynamics in such compounds, but this preliminary INS experiment confirms at least the presence of reorientations already inferred from NMR studies on WO_3,H_2O (*12*) but also on $WO_3,\frac{1}{3}H_2O$ (*33*).

(3) $WO_3,2H_2O$

In the absence of crystal diffraction study of $WO_3,2H_2O$, the analysis of its vibrational spectra will be based on the structural data available for $MoO_3,2H_2O$ (*7, 8*) since the two structures have been shown to be very similar (*6*).

Figure 1d compares the results obtained on $MoO_3,2H_2O$. They present only minor differences in the description of the layers of octahedra and predict four kinds of terminal Mo=O groups in the unit cell, with values of 1.680, 1.683, 1.691, and 1.722 Å.

The presence of three infrared absorptions at 1007, 945, and 918 cm^{-1} and of one intense Raman line at 960 cm^{-1} for $WO_3,2H_2O$ (Fig. 6, Table I) can thus be explained by the existence of four distinct W=O bonds. Nevertheless, the great difference of intensity distribution between the two spectroscopies indicates that these terminal bonds are certainly not vibrationally independent. The description of their dipolar coupling would of course be dependent on the kind of geometrical disposition which is retained (Fig. 1d).

The spectral density corresponding to the stretching modes ν(O–W–O) of the bridging oxygens is narrower and more structured than for WO_3,H_2O but again clearly distinct from m-WO_3 because of a general frequency lowering. As for WO_3,H_2O, this effect and the presence of a terminal ν(W=O) frequency constitute the more characteristic differences between a structure made of octahedra layers or of tridimensionally corner-sharing octahedra.

Below 500 cm^{-1} a larger number of bands than for WO_3,H_2O is detected, especially in the infrared spectra at 77 K (Fig. 6, Table I). The existence of two kinds of water molecules in $WO_3,2H_2O$ explains this multiplicity but it would be difficult without deuteration effects to propose a precise assignment. Nevertheless, we tentatively situate the ν(W–OH_2) mode at ~380 cm^{-1}. Indeed at this frequency a well defined Raman line is observed which could be the counterpart of the intense ν(W=O) vibration at 960 cm^{-1}. If several kinds of W–OH_2 bonds exist in parallel with the four distinct W=O bonds per unit cell, one can infer that several ν(W–OH_2) infrared bands splitted by dipolar coupling occur in the 350- to 400-cm^{-1} spectral region.

Actually, the $MoO_3,2H_2O$ structure (*7, 8*) indicates the presence of a wide range of OH···O angles and distances. They result from the rather complicated hydrogen bond network formed by the coordinated and interlamellar water molecules.

A rough classification in terms of families of hydrogen bond distances can be established. Coordinated water is involved in slightly stronger hydrogen bonds than in

WO_3,H_2O as shown by the family of $OH\cdots O$ distances (2.74 ± 0.04 Å) derived from $MoO_3,2H_2O$. The new intense absorption at 3160 cm^{-1} observed in the infrared spectrum of $WO_3,2H_2O$ can be assigned to the ν(OH) stretching modes of this family. The other new absorption at 3530 cm^{-1} may also be easily assigned to weak bifurcated hydrogen bonds formed by one OH bond of interstitial H_2O ($OH\cdots O = 3.14 \pm 0.06$ Å).

Finally, a third family of $OH\cdots O$ distances responsible for the intermediate absorption band at 3370 cm^{-1} is produced by the second OH bond of interstitial H_2O linked to an unshared oxygen of the next layer ($OH\cdots O = 2.82 \pm 0.04$ Å).

This is certainly a rather qualitative assignment of the infrared ν(OH) absorption pattern since we have arbitrarily grouped the hydrogen bonds in three families.

As for WO_3,H_2O, splittings are for example observed at 77 K in the higher-frequency subband. They can result from the separation of symmetric/antisymmetric modes of a given OH_2 molecule or from the resolution of further distinct OH group. The deformation mode δ(OH) also gives a very broad infrared band centered at about 1590 cm^{-1} with no apparent substructure.

(4) *h*-WO_3

As pointed out above, there are strong discrepancies between the few published spectra of *h*-WO_3 (*19, 21*). One can suppose that there is an inversion between Figs. 1a and b in (*19*). Indeed, the actual Raman spectrum of *h*-WO_3 presents strong lines at 817, 253, and 108 cm^{-1} and medium lines at 690 and 162 cm^{-1} which are clearly differentiated, as expected, from the *m*-WO_3 spectrum (Figs. 2 and 3, Table I). Nothing is detected around 950 cm^{-1} in agreement with the absence of terminal W=O groups.

The infrared spectrum of *h*-WO_3 present broad absorptions at 1000–600 and 400–200 cm^{-1} and a much narrower band at 440 cm^{-1}. The latter could well be specific of a deformation of the W–O–W bridge in the hexagonal arrangement of octahedra.

It must be noted that, apart from this specific band and the frequency differences with *m*-WO_3, the intensity distributions for *h*-WO_3 resemble much more those of *m*-WO_3 than those of the layered hydrates.

(5) $WO_3,\frac{1}{3}H_2O$

The infrared spectrum of $WO_3,\frac{1}{3}H_2O$ has already been partly discussed in connection with the presence of adsorbed water and OH groups (*9*). A subsequent wide-band proton NMR study as a function of temperature and degassing conditions has concluded that this compound can easily retain adsorbed surface water under the form OH_2 or OH (*33*).

The infrared spectrum of $WO_3,\frac{1}{3}H_2O$ corresponds to a sample not completely desorbed by vacuum treatment at 175°C. The comparison of the infrared spectrum before and after degassing clearly indicates that the bands at 1410 and 3220 cm^{-1} are due to adsorbed species. The former cannot be assigned to water deformation. On the other hand, OH groups would be expected to give ν(OH) and δ(OH) vibrations respectively at lower and higher frequencies. So, we think that before desorption we see the result of atmospheric water reaction on surface W=O groups to give W–OH bonds rather strongly associated with further water molecules 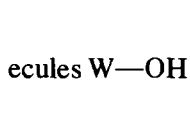 . All the W=O surface groups may not have reacted as indicated by a band at 1000 cm^{-1} which remains even after degassing.

Thus, $WO_3,\frac{1}{3}H_2O$ seems to be more sensitive than the other hydrates to the action of atmospheric water.

After degassing, the intrinsic structural properties of $WO_3,\frac{1}{3}H_2O$ are reflected by

the presence of a band at about 950 cm^{-1} in the infrared and Raman spectra (Fig. 7). It can be assigned to W=O terminal groups but its position would suggest a slightly shorter length than the value of 1.8 Å (9). On the basis of a W–O bond length of 2.1 Å for the $W-OH_2$ interaction it is also difficult to situate the corresponding stretching vibration in the 450–550 cm^{-1} range where no infrared absorption is present. Again we suspect the $W-OH_2$ distance to be in the 2.3 Å range.

It must be recalled that the structure has been established from X-ray powder diffraction data and the powder diffraction intensities are not very sensitive to oxygen atom positions. Therefore the bond-lengths given in (9) are approximate and greater confidence can be given in this particular case to the spectroscopic results.

The infrared absorption at 420 cm^{-1} seems to be due to a W–O–W mode of the hexagonal arrangement in h-WO_3.

The two Raman lines at 805 and 680 cm^{-1} can be assigned to stretching vibrations of the bridging oxygens. They are nearly at the same position as for h-WO_3 but broader, possibly as a result of the presence of two kinds of octahedra.

The structural water is characterized by its ν(OH) maximum at 3500 and δ(OH) at 1609 cm^{-1}. These values indicate that the OH bonds are only slightly perturbed by interlayer OH···O hydrogen bonds. The H_2O librations are difficult to distinguish from the octahedra deformations in the 450- to 300-cm^{-1} range. Only a broad and weak band is detected at ~325 cm^{-1} in the Raman spectrum. It might be due to $\nu(W-OH_2)$.

Let us note finally that the general shape of the $WO_3,\frac{1}{3}H_2O$ Raman spectrum (Fig. 7) lies in between those of the tridimensional m-WO_3 and h-WO_3 networks and of the two-dimensional layered hydrates as expected from its intermediate kind of structure.

(6) General Considerations

The infrared spectra are broad for all the powdered samples studied. This may partly be due to surface modes.

However, infrared absorption remains the best adapted technique to characterize the water vibrations and the eventual hydoxyl groups. Furthermore, the terminal W=O vibrators can also clearly be detected.

The Raman spectra below 1200 cm^{-1} present detailed features which reflect more clearly the structural characteristics of the octahedra arrangements. The qualitative differentiation that we have deduced between two and three-dimensional octahedra networks could certainly be rationalized with a force field calculation based on the different structures and on a polarization analysis of the Raman spectra of the crystals.

The values of the more characteristic infrared and Raman bands are summarized in

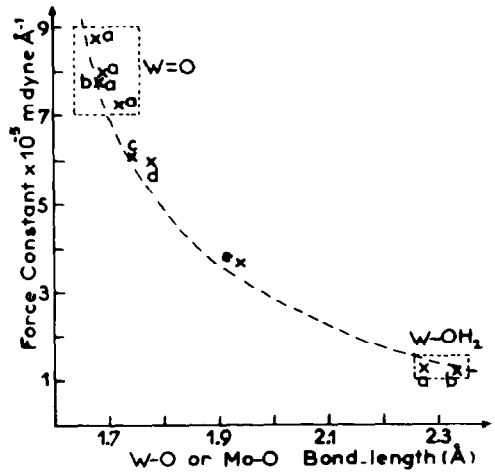

FIG. 10. Correlation between the force constant and the length of the W–O bond. (a) $WO_3,2H_2O$; (b) WO_3,H_2O; (c) $CaWO_4$; (d) $PbWO_4$; (e) $W_6O_{19}^{2-}$. The broken line reproduces the correlation established by Cotton and Wing (22) for the Mo–O bond. The W–O stretching frequency (cm^{-1}) can be calculated from the force constant by the expression: $\nu = 1.0729\sqrt{k}$. (k mdyne $Å^{-1}$).

Table I. One can also use published values for some specific systems such as $W_6O_{19}^{2-}$ (*35*), $CaWO_4$ (*39*), or $PbWO_4$ (*40*) to establish a relationship between force constant and length for the tungsten–oxygen bond. The experimental points, ranging from r(W–O) = 1.68 to 2.34 Å for k values respectively of about 8.8 to 1.2 10^5 mdyne/Å are reported in Fig. 10. The amount of data for intermediate values is too small for a precise correlation but it can be remarked that the curve previously established for Mo–O by Cotton and Wing (*22*) fits well the available W–O points.

Therefore, it can be concluded that these two systems behave in a very similar way and this gives weight to the W–O relationship. Such a correlation is a useful starting point for the analysis of the mixed valence colored molybdenum or tungsten oxydes (*41*).

Conclusion

The primary aim of this work was to provide a clear spectral identification of *m*-WO_3, *h*-WO_3, WO_3,H_2O, $WO_3,2H_2O$, and $WO_3,\frac{1}{3}H_2O$. Until now, these compounds had only been partially investigated, sometimes without control of the laser power in Raman and without precise research of the water vibrations in the infrared.

We show that each compound has a specific distribution of intensity and frequency for the bridging W–O–W bonds. A correlation between the frequency and bond-length of the W–O bond has been established. It is confirmed that the shorter bonds (~1.7 Å) correspond to terminal W=O oscillators which give well defined infrared or Raman bands around 950 cm^{-1}. The W–OH_2 bonds (~2.3 Å) are characterized by a stretching mode arizing around 380 cm^{-1}. Strong similarities exist between the W–O and Mo–O compounds.

NMR and INS data lead to the conclusion that in the hydrates WO_3,xH_2O, coordinated water molecule execute hindered rotations. This coordinated water can be clearly differentiated from interlamellar water and surface hydroxyl groups by analysis of the infrared spectra.

References

1. B. O. Loopstra and H. M. Rietveld, *Acta. Crystallogr. Sect. B* **25,** 1420 (1969).
2. R. Diehl, G. Brandt, and E. Salje, *Acta. Crystallogr. Sect. B* **34,** 1105 (1978).
3. B. Gerand, G. Nowogrocki, J. Guenot, and M. Figlarz, *J. Solid State Chem.* **29,** 429 (1979).
4. P. Hagenmuller, *in* "Progress in Solid State Chemistry" (H. Reiss, Ed.), Vol. 5, p. 71, Elmsford, NY (1971).
5. J. T. Szymanski and A. C. Roberts, *Can. Mineral.* **22,** 681 (1984).
6. J. R. Günter, *J. Solid State Chem.* **5,** 354 (1972).
7. S. Åsbrink and B. G. Brandt, *Chem. Scripta* **1,** 169 (1971).
8. V. B. Krebs, *Acta Crystallogr. Sect. B* **28,** 2222 (1972).
9. B. Gerand, G. Nowogrocki and M. Figlarz, *J. Solid State Chem.* **38,** 312 (1981); B. Gerand, Thesis, Amiens, FRANCE, 1984.
10. E. Salje, *Acta Crystallogr. Sect. A* **31,** 360 (1975).
11. V. I. Spitzin and V. J. Kabanow, *Z. Anorg. Allg. Chem.* **322,** 248 (1963).
12. V. Ya Kabanov and V. F. Chuvaev, *Russ. J. Phys. Chem.* **38,** 717 (1964).
13. W. Krasser, *Naturwissenschaften* **56,** 213 (1969).
14. C. Rocchioli-Deltcheff, *C. R. Acad. Sci. B* **268,** 45 (1969).
15. I. R. Beattie and T. R. Gilson, *J. Chem. Soc. (A),* 2322 (1969).
16. R. Mattes and F. Schröder, *Z. Naturforsch. B* **24,** 1095 (1969).
17. G. M. Ramāns, J. V. Gabrusenoks, and A. A. Veispals, *Phys. Status Solidi A* **74,** K41 (1982).
18. V. I. Gavrilyuk and I. M. Chernenko, *Inorg. Mat.* **18,** 993 (1982).
19. R. Mercier, O. Bohnke, C. Bohnke, G. Robert, B. Carquille, and M. F. Mercier, *Mater. Res. Bull.* **18,** 1 (1983).
20. M. Pham Thi and G. Velasco, *Solid State Ionics* **14,** 217 (1984).
21. M. Pham Thi and G. Velasco, *Rev. Chim. Min.* **22,** 195 (1985).
22. F. A. Cotton and R. M. Wing, *Inorg. Chem.* **4,** 867 (1965).
23. J. C. J. Bart, F. Cariati, and A. Sgamelotti, *Inorg. Chim. Acta* **36,** 105, 261 (1979).

24. L. ABELLO, E. HUSSON, Y. REPELIN, AND G. LUCAZEAU, *Spectrochim. Acta A* **39,** 641 (1983).
25. Y. REPELIN, E. HUSSON, L. ABELLO, AND G. LUCAZEAU, *Spectrochim. Acta A* **41,** 993 (1985).
26. M. L. FREEDMAN, *J. Amer. Chem. Soc.* **81,** 3834 (1959).
27. K. FURUSAWA AND S. HACHISU, *Sci. Light (Tokyo)* **15,** 115 (1966).
28. Neutron Beam Facilities at the HFR, Institut Laue-Langevin, Grenoble, France.
29. A. J. DIANOUX, R. E. GHOSH, H. HERVET, AND R. E. LECHNER, Internal Report 75D16T, ILL, Grenoble, 1975.
30. See, for example, "Electromagnetic Surfaces Modes" (A. D. Boardman, Ed.), Wiley, New York, 1982.
31. C. PIGENET AND F. FIEVET, *Phys. Rev. B* **22,** 2785 (1980).
32. L. MARTY, Thesis, University Paris VI, 1972.
33. C. DOREMIEUX-MORIN, L. C. DE MENORVAL, AND B. GERAND, *J. Solid State Chem.* **45,** 193 (1982).
34. M. FALK AND O. KNOPP, *in* "Water: A comprehensive Treatise" (F. Franks, Eds.), Vol. 2, p. 55, Plenum, New York, 1973.
35. V. R. MATTES, H. BIERBÜSSE, AND J. FUCHS, *Z. Anorg. Allg. Chem.* **385,** 230 (1971).
36. M. BEE AND C. POINSIGNON, "Application of Quasielastic Neutron Scattering to Solid State Chemistry. Biology and Material Science," Adams & Hilger, London (1966).
37. B. PEDERSEN, *J. Chem. Phys.* **41,** 122 (1964).
38. W. ECKERS AND H. D. LUTZ, *Spectrochim. Acta A* **41,** 1321 (1985).
39. R. K. KHANA AND E. R. LIPPINCOT, *Spectrochim. Acta A* **24,** 905 (1968).
40. W. P. GRIFFITH, *J. Chem. Soc. (A)* 286 (1970).
41. F. CARIATI, J. C. J. BART, AND A. SGAMELLOTTI, *Inorg. Chim. Acta* **48,** 97 (1981).